Defect structures in silver chloride

2004 J. Phys.: Condens. Matter 16 S2827

(http://iopscience.iop.org/0953-8984/16/27/016)

INSTITUTE OF PHYSICS PUBLISHING JOURNAL OF PHYSICS: CONDENSED MATTER

J. Phys.: Condens. Matter **16** (2004) S2827–S2838 PII: S0953-8984(04)73590-0

Defect structures in silver chloride

D J Wilson, A A Sokol, S A French and C R A Catlow

Davy Faraday Research Laboratory, The Royal Institution of Great Britain, 21 Albemarle Street, London W1S 4BS, UK

E-mail: dan@ri.ac.uk

Received 15 December 2003, in final form 23 February 2004
Published 25 June 2004
Online at stacks.iop.org/JPhysCM/16/S2827
doi:10.1088/0953-8984/16/27/016

Abstract

We report a study of the atomic and electronic structure, along with spin densities and energetics, of the primary intrinsic defects in silver chloride in their neutral and charged forms. We have correctly predicted the dominance of the cation Frenkel defect. In agreement with recent studies we have found that both the neutral and charged silver interstitial defects adopt a split-interstitial geometry, with the conventional body-centred interstitial found to be a transition state. We propose that the split-interstitial structure forms four-membered chains which can migrate through the crystal by a knock-on mechanism. We have also studied the structures of the cation and anion vacancies, and seen little relaxation, except on formation of an F-centre, where there is an unusually strong contraction of the nearest-neighbour cations towards the vacant site, which has been proposed to be an ion-size effect.

1. Introduction

The existence of structural defects in silver chloride has long been known to be essential to the photographic process [1, 2]. Frenkel pairs, created when silver ions move from their lattice sites to nearby interstitial positions, are prevalent in the crystalline lattice [3]. On excitation by actinic light, electron–hole pairs (excitons) are formed. The electrons are thought to become trapped at surface sites, and exert an electrostatic force on the positively charged interstitial ions. Consequently these ions migrate towards the surface, at which point they are reduced to form atomic silver. Clusters of these atoms then catalyse the reduction of the entire crystal to metallic silver by the developer solution.

Owing to their industrial importance, the properties of the defects have been studied in detail. Schottky pairs (cation–anion vacancy pairs) dominate in the alkali halides. In the silver halides, however, cation Frenkel defects are more abundant than Schottky defects [4], with experimental formation energies of 1.45 eV [5] and 1.5–2.4 eV [4] respectively, the uncertainty in the latter being due to the difficulty in measuring the properties of minority defects. It is

also known that the interstitial ion can migrate exceptionally easily through the solid, having a barrier to migration of only 0.04 eV [6, 7].

The electronic properties of the material are also of great importance. For the photographic process to work efficiently it is desirable that the electron–hole pair is prevented from recombining. Dopants are often added to the crystal to trap the hole, allowing the electron to combine with the interstitial ion to form the neutral silver atom. The properties of the hole are therefore of great technological importance, but are also of fundamental scientific interest as they help to illuminate the properties of the unusual valence band of the material [3]. In the presence of the Madelung field, the chloride 3p level coincides with the silver 4d level to within 1 eV [8]. Inversion symmetry prevents hybridization of the two states at the Brillouin zone centre, but not at the zone boundaries, which has the effect of producing an inverted valence band, with a maximum at the L-point $(\frac{1}{2}, \frac{1}{2}, \frac{1}{2})$ of the Brillouin zone.

Early conductivity measurements [9, 10] showed that electron–hole recombination in cadmium-doped silver halides was inhibited by the vacancies introduced by the divalent dopant. These vacancies effectively bear a negative charge and hence would attract nearby holes. Optical experiments [11] on the same material showed that the concentration of self-trapped holes (STH) decays above 50 K. However, a signal persists above this temperature which was attributed to an STH perturbed by a neighbouring cation vacancy. Further electron paramagnetic resonance (EPR) studies of cadmium-doped silver chloride have shown the existence of an STH localized on a single silver cation with a Jahn–Teller elongation along the [100] axis, bound to a cation vacancy site, which is stable up to 110 K [12]. More recently, electron nuclear double resonance (ENDOR) spectroscopy has been used to study the distribution of the hole in more detail [13]. This study concurs that the hole is centred on a single silver cation, but has determined that only 19% of the spin density is located on this centre. The remainder is largely on the 3s and 3p orbitals of the equatorial chloride anions. Their data do not, however, suggest the proximity of a cation vacancy, as they find that the d_{4h} symmetry of the silver $4d_{x^2-y^2}$ orbital is intact. However these experiments were all carried out at 1.2 K, a temperature at which unperturbed STHs may dominate.

The photoelectron can also become trapped, which occurs preferentially at a surface kink site which bears an effective positive charge of $+\frac{1}{2}e^-$ [14], but may also happen within the bulk, forming a shallow electron centre (SEC). Early work by Sakuragi [15] suggested that the photoelectron binds to the positively charged interstitial cations in the material. However, optical and EPR spectroscopy failed to determine the structure of the centre.

Recently, Bennebroek *et al* [16, 17] have used ENDOR spectroscopy to study this problem. They have determined the structure to be a Ag_2^+ molecular ion within the crystal, centred on a lattice site. This dimer could be orientated in a [111], [110] or [100] direction. On the grounds of symmetry, they concluded that the dimer is orientated either along a [110] or [100] direction. Due to the additional free space available to the ions, the [110] direction was considered more favourable. The authors have shown the electron to be trapped diffusely, and have suggested that on its removal to form the charged defect, the geometry will change very little.

The nature of both hole and electron states in AgCl, and their interaction with point defects, clearly poses problems which present a challenge to theoretical methods. Early defect calculations on the silver halides relied upon atomistic interatomic potential methods [18–25] and could only be applied to closed-shell (charged) defects, for which they reveal, of course, no information on electronic structure. They did, however, give valuable results on defect structure, formation and migration energies.

To date, electronic structure methods have been used to study the perfect material [26–34]. Good qualitative agreement has been found with experimental band structures and density of states. Baetzold and Eachus [35] have applied Hartree–Fock based embedded-cluster

techniques to study the Ag_2 split-interstitial species. However, there has not been a thorough study of intrinsic point defects in bulk AgCl.

In this work we use density functional theory (DFT), electronic structure calculations, with periodic boundary conditions, to study the atomic and electronic structure first of neutral point defects in silver chloride. We then compare the energies of the corresponding charged species with results of previous semiclassical calculations that employed the Mott–Littleton approach [19, 25]. Our approach, although state-of-the-art, suffers some fundamental limitations. Current implementations of DFT tend to over delocalize electron density and systematically underestimate band gaps [36–38]. Spin–orbit splittings might be of importance, but are completely omitted in our treatment. These limitations affect electronic excitations, but can be expected to be less significant for the defect energies and structure, the primary objectives of this paper.

2. Methodology

This study was performed using DFT, as implemented in the CASTEP [39] code, which employs periodic boundary conditions, a plane-wave basis set and pseudopotentials. The GGA density functional of Perdew, Burke and Ernzerhof (PBE) [40] was chosen for its accuracy and numerical stability. This method is advantageous for the study of point defects in ionic materials as it treats all regions of space with an equal weighting; giving vacancies the same level of description as the constituent ions, and allowing for an accurate representation of trapped electrons.

Ultrasoft pseudopotentials derived using the PBE functional, and containing relativistic effects, were used for all calculations, having core and valence regions consisting of $[Kr]4d^{10}5s^1$ and $[Ne]3s^23p^5$ for silver and chlorine respectively [39, 41]. A thorough study of the effect of basis set truncation was performed, and it was found that while truncation of the basis set at 300 eV leads to only a marginal error for the pure material, a cut-off of 350 eV is required for an adequate description of defect states. These calculations reproduce the experimental lattice parameter of AgCl to within $\frac{1}{2}\%$. All of the following defect calculations were performed with a fixed lattice parameter $a = 5.533$ Å, with this value taken from the initial relaxed calculation.

As an additional test, the gas-phase dimers AgCl, Ag_2 and Cl_2 were modelled with CASTEP, maintaining periodic boundary conditions by placing each dimer in an empty unit cell of sufficient size to isolate the dimer from its images. For ease of comparison, a cubic cell with a lattice parameter equal to that of our AgCl supercell described below was chosen ($a = 11.066$ Å). The results of these calculations are tabulated in table 1, along with corresponding experimental results. While the bond lengths are in good agreement (within 2% of experimental values) the bond dissociation energies are less well described (within 15%). However, the energies of both AgCl and Ag_2 are accurate to within 0.15 eV, which should lead to minimal error for the defect systems studied here.

All calculations were performed using a cubic $2 \times 2 \times 2$ supercell containing 64 ions, of which only the inner 27 were allowed to relax, leaving the boundary atoms fixed. When present, the defect was placed near the centre of the cube. Symmetry was imposed on the cell when appropriate, to reduce computational expense. The effects of supercell size were not studied as the calculations were already expensive on computing resources. However, our tests employing interatomic potentials show that this cell is sufficient to account for major structural relaxation around the defects in question. A proper description of electronic effects may, however, require a larger cell. It has recently been shown, for example, that contamination

Table 1. Dimer properties calculated using CASTEP.

	Bond length (Å)		Dissociation energy (eV)	
Dimer	This work	Experiment	This work	Experiment
Ag_2	2.584	2.531 [42]	1.748	1.634 [43]
Cl_2	1.983	1.988 [44]	2.899	2.510 [45]
AgCl	2.293	2.281 [44]	3.199	3.239 [46]

of the local potential by that of the periodic images can affect the ionization potential of an F-centre in a 64-site supercell of NaCl by 0.8 eV [47].

When modelling aperiodic systems within periodic boundary conditions, the choice of k-point sampling in the first Brillouin zone is critical [48]. A good choice can accelerate convergence with supercell size by minimizing defect–defect interactions. Following Makov *et al* [48] we chose a set containing four $(\frac{1}{4}, \frac{1}{4}, \frac{1}{4})$-type k-points, which our tests show to produce converged results. For the split-interstitial system ($R\bar{3}m$) symmetry reduces the set to two unique points, while for the vacancy systems ($Pm\bar{3}m$) the set is reduced to a single point in reciprocal space.

We calculate properties of isolated vacancy and cation interstitial defects in their neutral and charged states. When charged defects were studied, a uniform charge-neutralizing background was applied. This approach leads to an error due to the electrostatic interactions between the charge and its images, which was corrected for using the term derived by Leslie and Gillan [49]. The individual defect formation energies are then calculated according to:

$$E_f(Q) = E_{def} - E_{pure} - n_{Ag}\mu_{Ag} - n_{Cl}\mu_{Cl} + Q\mu_e + E_{corr}(Q), \tag{1}$$

where E_{def} is the energy of the defective cell, E_{pure} is the energy of the defect-free reference system, $n_{Ag/Cl}$ are the change in number of cations/anions on going from the pure cell to the defective system, $\mu_{Ag/Cl}$ are the cation/anion chemical potentials relative to their standard states, Q is the net cell charge, μ_e is the chemical potential of the electron and E_{corr} is the Leslie–Gillan correction described above.

The chemical potential of the electron, or equivalently the Fermi energy, is undefined in a perfect insulator such as silver chloride [50], and hence calculation of charged defect formation energies is problematic. For the uncharged defects, the chemical potentials of silver and chlorine were calculated relative to their standard states. For silver, the energy was obtained from a fully converged calculation of metallic silver, using the same pseudopotential and functional. For chlorine, the chemical potential is half the absolute energy of the optimized Cl_2 dimer described above (see table 1).

When calculating the full reaction cycle (i.e. the formation of a pair of charge-compensating defects) two such equations are combined. For the cases of the cation Frenkel and Schottky defects, the resulting equations are:

$$\Delta E \text{ (Frenkel)} = E_{def}(Ag_I) + E_{def}(V_{Ag}) - 2E_{pure} + 2E_{corr}(Q), \tag{2}$$

$$\Delta E \text{ (Schottky)} = E_{def}(V_{Ag}) + E_{def}(V_{Cl}) - \left(2 - \frac{1}{N}\right)E_{pure} + 2E_{corr}(Q), \tag{3}$$

where N is the number of AgCl formula units in the pure cell, and all other terms are as described above.

The correction term appears twice in the formulae as it is proportional to the cell charge squared, and thus both defect cells contribute equally. For the Schottky pair, it is assumed the removed ions combine and add to the bulk material, and hence the sum of their chemical

Table 2. Defect formation energies for AgCl (eV).

	This work		Interatomic potentials [25]	Experiment
	Neutral	Charged	(charged)	(charged)
Silver interstitial	2.00	—	−5.42	—
Silver vacancy	0.37	—	6.88	—
Chloride vacancy	1.53	—	4.35	—
Silver Frenkel pair	2.37	0.58	1.46	1.45 [5]
Schottky pair	1.08	0.79	1.70	>1.5 [4]

potentials can be replaced with the energy of a pair of ions in the bulk. The dependence on the electron chemical potential is cancelled, and thus calculation of these energies is tractable regardless of charge state.

The energies obtained in all calculations are defined relative to the valence band maximum. In a defective system, states are introduced into the band gap, changing this reference energy. Consequently, a shift is introduced which must be corrected for. One method of achieving this is to compare the electrostatic potential at a distance from the defect with that of the pure bulk material [51]. Alternatively, comparison of the energies of unaltered semi-core states in the band structures may suffice [52]. This matter is currently under investigation, as it is expected to provide a noticeable contribution to the defect energetics calculated with the current $2\times2\times2$ supercell, although it is likely to be less important for larger cells.

3. Energies of defect formation

Our intention is to elucidate the electronic and structural properties of the fundamental defect pairs in silver chloride. Initially, we have studied the energetics of formation of individual neutral and charged defects in the limit of infinite separation.

Calculations on the neutral species are more accurate as they require fewer correction terms. They also yield useful information on the localization of the excess hole or electron.

We have thus first considered three processes:

- Adding a silver atom to form an interstitial defect (which can be considered as an Ag^+ cation and an excess electron):

$$\mathrm{Ag(s)} \longrightarrow \mathrm{Ag}_\mathrm{I}^\bullet + \mathrm{e}^-. \tag{4}$$

- Removing a silver atom leaving a vacancy and an excess hole:

$$\mathrm{Ag}_\mathrm{Ag} \longrightarrow V'_\mathrm{Ag} + h^+ + \mathrm{Ag(s)}. \tag{5}$$

- Removing a chlorine atom resulting in a chlorine vacancy and an additional electron:

$$\mathrm{Cl}_\mathrm{Cl} \longrightarrow V_\mathrm{Cl}^\bullet + \mathrm{e}^- + \tfrac{1}{2}\mathrm{Cl_2(g)}. \tag{6}$$

Chlorine interstitial defects were not considered as their concentration is known to be negligible.

The resulting defect energies are reported in table 2, which gives both the individual energies and the corresponding values for the neutral Frenkel and Schottky pairs.

Next we considered the charged defects, in which the excess electron or hole has been removed to leave an entirely closed-shell system. These are the species previously studied by Mott–Littleton based atomistic modelling and conductivity measurements. The energies of

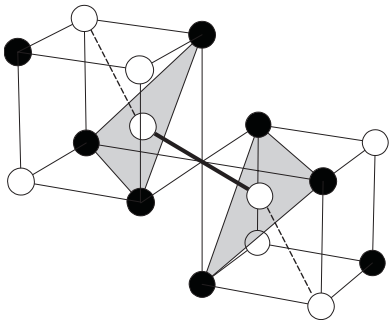

Figure 1. Illustration of the Ag_2^{2+} split-interstitial species in the [111] orientation, with a typical cation chain highlighted. White circles represent silver ions, black represent chloride ions.

the Frenkel and Schottky defects are also shown in table 2. However, the individual defect formation energies are ill-defined, for the reasons stated in section 2, and are therefore omitted.

It can be seen from the table, that the dominance of the charged Frenkel species is correctly predicted. However, both values are lower than experiment, which is likely to be due to both the supercell size and the inherent deficiencies of the density functional. Calculations on larger cells are underway, and will be reported in a subsequent publication.

It is interesting to note that DFT correctly predicts the ordering of these defects. There has been much debate over the last 25 years over the origin of the unique properties of the silver halides, including the predominance of the cation Frenkel defect [53]. It was previously thought that interatomic van der Waals forces stabilize the silver interstitial, lowering the Frenkel energy. DFT methods cannot model accurately the long range van der Waals attraction, but as we have shown, still predict the dominance of this form of defect.

4. Atomic structure and spin localization

4.1. Silver interstitial species

The atomic structure of the interstitial defect is of considerable interest. Most previous analyses assumed the charged interstitial ion to be at a body-centred (BC) site. Energetics from atomistic calculations on charged interstitials supported this assumption [19, 25], and it became the model with which all subsequent experimental data were interpreted.

Our calculations have shown the BC structure to be unstable. Instead, we have found the equilibrium configuration to involve a second cation, forming a dumb-bell-shaped split-interstitial structure centred on a lattice site (see figure 1), in agreement with the Hartree–Fock results of Baetzold and Eachus [35] and the ENDOR work of Bennebroek *et al* [16, 17]. There is, however, disagreement over the orientation of this species. Based on symmetry arguments, Bennebroek suggests a [110] orientation for the neutral defect. However, our calculations show that the [111] orientation is more stable. We find the difference in energy of the two orientations to be 0.4 eV. Simple steric arguments suggest that the [111] orientation would be expected to be more favourable, which is, indeed, the model Baetzold used for his Hartree–Fock calculations.

As is common when dealing with H-centres in the alkali halides, the split-interstitial species can be treated as a molecular dimer within the crystal [54]. We find the bond length of the charged Ag_2^{2+} dimer to be 2.95 Å in the crystal, with the silver ions located at the centres of two triangles of chloride ions, as shown in figure 1. The distance between each member of the dimer and its nearest cation neighbours was found to be 2.94 Å. We therefore observe chains of

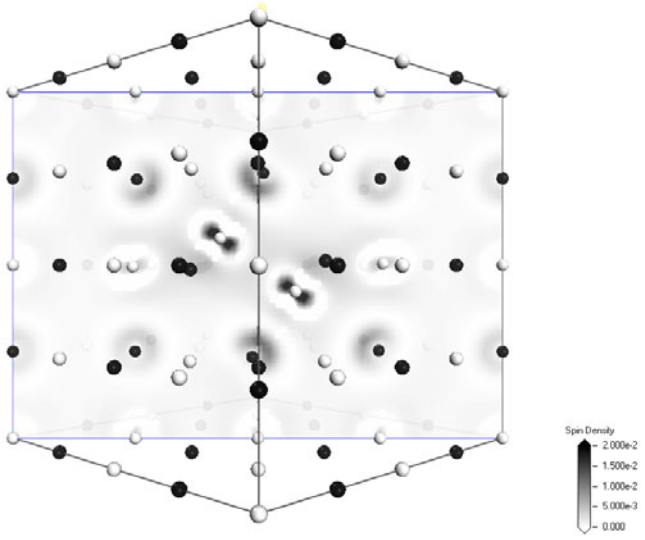

Figure 2. Spin localization in defective AgCl: silver interstitial. Contour plot of the (100) plane containing the Ag_2^+ species (centre). White spheres silver, black spheres chlorine.

cations with approximately equal separation (indicated in figure 1), suggesting the importance of electrostatics in determining the structure. The slight inequality in the bond lengths is likely to be due to electrostatic interactions with the surrounding chloride anions. These are situated at a distance of 2.49 Å from each cation (0.28 Å shorter than normal separation in pure AgCl, but with silver in a trigonal configuration rather than octahedral), displaced only slightly from their lattice sites (0.02 Å outwards) due to the competition between Coulombic attraction and Pauli repulsion.

To validate this analysis we performed calculations purely of the electrostatic energies. Atomic coordinates from our DFT calculations were imported into the GULP code [55], and assigned full ionic charges. Variation of the electrostatic energy was measured as a function of the Ag_2^{2+} dimer bond length, while keeping the rest of the crystal fixed. This procedure gave an equilibrium bond length of 2.9 Å, which is consistent with our *ab initio* data, confirming that electrostatic interactions control the structure of this system. Our tests on the molecular dimer reported in section 2 allow us to say that the interaction between silver cations at closer separation is well described, and hence we believe the split-interstitial geometry to be valid.

On trapping an electron to form the neutral Ag_2^+ defect, it may be expected that the dimer becomes bonded due to the presence of an electron in the σ_g bonding orbital, in analogy with the molecular model above. However, we find the trapped electron to be very diffuse in agreement with the aforementioned ENDOR experiments which, based on effective mass theory, predict a Bohr radius of 17.2 Å [16], which causes only a small perturbation to the system, leading to a small increase in the dimer bond length to 3.00 Å. The spin density for the system can be seen in figure 2. Further comparison with experiment would require calculations on a larger supercell capable of fully enclosing the electron density. It should be noted that some caution in the interpretation of our results is needed. DFT is well known to over-delocalize the electron distribution [38], which may have the effect of increasing the bond length of the molecular ion in the neutral state, making the more constrained [110] geometry less favourable.

Our calculated equilibrium structure closely resembles the transition state for the collinear interstitialcy migration mechanism proposed in previous analyses [20, 56]. In this process, a

Table 3. Inward displacement of shells of nearest-neighbour (NN) ions towards silver or chlorine vacancies (Å).

		1st-NN	2nd-NN	3rd-NN
Silver vacancy	Charged	−0.098	+0.059	−0.023
	Neutral	−0.087	+0.066	−0.040
Chloride vacancy	Charged	+0.043	+0.113	−0.017
	Neutral	+0.692	+0.080	+0.006

BC interstitial ion moves along a [111] direction displacing a neighbouring cation into a vacant interstitial site. The two states have long been known to have very similar energies. Early atomistic calculations found the BC geometry to be stable with a [111]-orientated transition state 0.03 eV higher in energy [24]. In contrast, our calculations have shown that the BC configuration is in fact a transition state, and the split-interstitial is a minimum. We calculated the difference in energy of the two species to be 0.023 and 0.064 eV for the neutral and charged species, respectively, both favouring the split-interstitial structure. As these values are comparable to thermal energies we would expect the cation chains described above to propagate easily throughout the crystal in three dimensions by a knock-on mechanism. By contrast, a [110]-orientated dimer would be restricted to a two-dimensional plane, reducing the efficiency of the photographic process.

At this stage, a detailed comparison with conductivity experiments is not possible as all experimental results have so far been analysed based on a body-centred model [6, 18, 57]. A variety of experimental and modelling techniques have now provided support for the split-interstitial structure. Consequently, a re-examination of the experimental data may be desirable. It is also possible that the application of post-Hartree–Fock methods may be required to study the effects of electron correlation on the subtle balance of energetics in the silver halides.

4.2. Silver vacancy

For the corresponding neutral cation vacancy, we observe small structural relaxations, as reported in table 3. In the closed-shell system containing the charged defect we find that the distance between the vacancy centre and nearest-neighbour chloride ions increases, while the nearest silver ions relax inwards, as would be expected on electrostatic grounds.

For the neutral defect, in which an excess hole is present, the extent of the structural relaxation of the next-nearest-neighbour cations is greater, while nearest-neighbour anions relax less. Examining the distribution of the hole in figure 3, it can be seen that it predominantly localizes on the silver cations, populating the $d_{x^2-y^2}$ orbitals. As a result, the cations become fractionally more positively charged, and thus are attracted to the negatively charged vacancy. This localization was found to be stable with respect to small symmetry-breaking perturbations of the nearest-neighbour ions. The spin density of the boundary cations is greater than those nearer the vacancy, suggesting that this supercell is not large enough to model the spin localization accurately.

Previous studies of the hole–vacancy complex have suggested that the hole is centred on a single Jahn–Teller elongated lattice cation adjacent to the vacancy [12, 58]. This difference in distribution may be due to the localization problem in DFT. Pacchioni *et al* have recently found that the hole in an α-quartz Al centre is incorrectly described by DFT [37]. Experiment and MP2 calculations showed localization on a single oxygen site, while hybrid and pure DFT methods showed the hole to be delocalized over a number of oxygen ions.

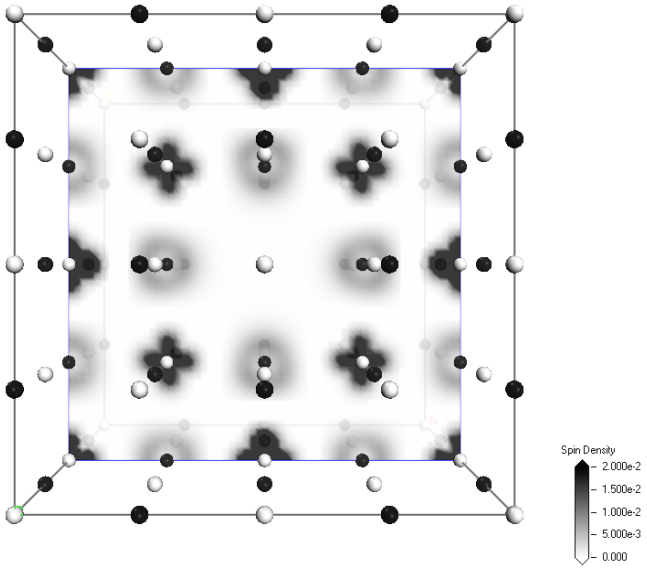

Figure 3. Spin localization in defective AgCl: silver vacancy. Contour plot of a (100) plane containing the vacancy (centre).

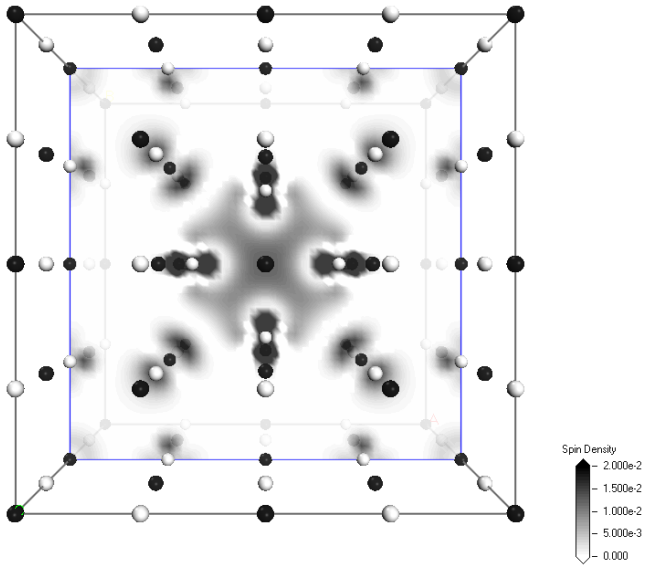

Figure 4. Spin localization in defective AgCl: chlorine vacancy. Contour plot of a (100) plane containing the vacancy (centre).

4.3. Chlorine vacancy

The properties of vacancies at anion sites are also of considerable interest. In the alkali halides, F-centres form, stabilizing the excited electron [54]. It can be seen in figure 4 that a diffuse F-centre also forms in AgCl. However, the electron is largely located upon the nearest-neighbour cations, rather than being centred on the vacancy itself as in a conventional F-centre.

Structural relaxation is minimal in the charged cell, with only small displacements from the bulk lattice positions, as can be seen in table 3. In contrast, the trapping of an electron causes the neighbouring silver ions to contract symmetrically into the vacancy by 0.69 Å. Again, the radial displacement of the other ions is small, which could, however, be due to the constraints imposed by the small size of the cell. When breaking the initial symmetry, the system relaxes back to the symmetrical geometry shown in the figure.

In the majority of systems studied in the literature [36, 54], the nearest-neighbour cations to the vacancy expand outwards. The unusual cation contraction observed in our calculations therefore warranted further examination. As a test of the basis set used, we employed the DFT code DMol3 [59], making use of an atom-centred numerical basis set and the PW91 exchange–correlation functional [60]. We repeated the calculation, and found the same structural relaxations as reported in table 3 to within 4%.

As a further test, we used our methodology to study a well-known and well-studied system. Sodium chloride (NaCl) was chosen due to its apparent similarities to AgCl, being isostructural with a common anion, and lattice parameters that match to within 0.1 Å. Using the same procedure as above we studied the F-centre, and found a well-localized electron contained within the vacancy, along with small structural relaxations, with the nearest-neighbour cations moving only 0.025 Å. On removal of this trapped electron to form a charged defect, we find outward relaxation of the cations and inward relaxation of the nearest anions, with magnitudes comparable with previous embedded-cluster calculations [61].

Analysis of the electron density of the two systems (AgCl and NaCl) reveals the explanation for their differing behaviours. Although the two materials have near identical lattice parameters, the silver ion has an ionic radius of 1.15 Å compared to that of sodium, 1.02 Å [62]. While NaCl exhibits close-packed-spherical ions, the constituent ions of AgCl are compacted along the bonds to produce a close-packed array of cuboids. Thus cations in the AgCl structure can be thought of as being under compression. On creation of a vacancy, this compression can be relieved by movement of the cations into the void. The large relaxation is not observed for the silver vacancy described above, as an alternative process, the electronic relaxation of the nearest-neighbour anions, can take place owing to their high electronic polarizability.

5. Summary

For the last 30 years, modelling defects in the silver halides has proved to be a major challenge to standard theoretical techniques. Previous studies using interatomic potential based methods have had considerable success, but required adjustments of the potential parameters in order to model defect behaviour accurately [19, 20, 25]. In this study we have used DFT methods to study the structural form of neutral and charged intrinsic point defects in AgCl.

We have correctly predicted the dominance of the cation Frenkel defect, and found a split-interstitial configuration of the cation to be favoured over the conventional body-centred interstitial defect, confirmed in this work as a transition state. Previous studies have suggested that strong van der Waals attraction stabilizes the interstitial, lowering the energy required to form a Frenkel pair. Our calculations suggest that this is unlikely, and that the atomic configuration of the interstitial centre may instead be the key factor.

Strong evidence, in terms of energetics and migration mechanisms, has been presented for the prevalence of the [111] orientation of the split-interstitial centre over the ENDOR-predicted [110] orientation. We have shown that the effect of electrostatics is the key factor in determining the structure of this centre, and that little molecular bonding occurs within the Ag_2 pair on addition of an electron to the system.

Small structural relaxation was found to occur around the cation vacancy in both its neutral and charged forms. For the neutral case, it was observed that the excess hole localizes on silver d orbitals. However, the exact nature of the localization will require further study, possibly employing post-Hartree–Fock methods; further experiments will also clearly be needed. Conversely, around the neutral anion vacancy the cations relax significantly, which we propose to be predominantly an ion-size effect.

Acknowledgments

We would like to thank J Gavartin, P Lindan and Th D Pawlik for useful discussions, and Accelrys Inc. for the use of their Materials Studio 2.2 modelling and visualization software. DJW would like to thank Eastman Kodak for funding. CRAC would like to thank M J Norgett, J Corish, P W M Jacobs and R Baetzold for their contributions to earlier work on defects in silver halides.

References

[1] Gurney R W and Mott N F 1938 *Proc. R. Soc.* A **164** 151–67
[2] Hamilton J F 1988 *Adv. Phys.* **37** 359–441
[3] Seitz F 1951 *Rev. Mod. Phys.* **23** 328–52
[4] Fouchaux R D and Simmons R O 1964 *Phys. Rev.* A **136** 1664–74
[5] Aboagye J K and Friauf R J 1975 *Phys. Rev.* B **11** 1654–64
[6] Corish J and Jacobs P W M 1972 *J. Phys. Chem. Solids* **33** 1799
[7] Batra A P and Slifkin L M 1975 *Phys. Rev.* B **12** 3473
[8] Basanni F, Knox R S and Fowler W B 1965 *Phys. Rev.* **137** 1217–25
[9] Cordone L and Palma M U 1966 *Phys. Rev. Lett.* **16** 22–5
[10] Cordone L, Fornili S L and Micciancio S 1969 *Phys. Rev.* **188** 1404–7
[11] Kanzaki H and Sakuragi S 1971 *Solid State Commun.* **9** 1667
[12] Kao C, Rowan L G and Slifkin L M 1990 *Phys. Rev.* B **42** 3142–51
[13] Bennebroek M T, Duijn-Arnold A V, Schmidt J, Poluektov O G and Baranov P G 2002 *Phys. Rev.* B **66** 054305
[14] Mitchell J W 1982 *Photog. Sci. Eng.* **26** 270–9
[15] Sakuragi S and Kanzaki H 1977 *Phys. Rev. Lett.* **38** 1302–5
[16] Bennebroek M T, Poluektov O G, Zakrzewski A J, Baranov P G and Schmidt J 1995 *Phys. Rev. Lett.* **74** 442–5
[17] Bennebroek M T, Arnold A, Poluektov O G, Baranov P G and Schmidt J 1996 *Phys. Rev.* B **54** 11276–89
[18] Hove J E 1956 *Phys. Rev.* **102** 915–6
[19] Catlow C R A, Corish J and Jacobs P W M 1979 *J. Phys. C: Solid State Phys.* **12** 3433–45
[20] Jacobs P W M, Corish J and Catlow C R A 1980 *J. Phys. C: Solid State Phys.* **13** 1977–88
[21] Jacobs P W M, Corish J and Devlin B A 1982 *Photog. Sci. Eng.* **26** 50–5
[22] Catlow C R A, Corish J, Harding J H and Jacobs P W M 1987 *Phil. Mag.* A **55** 481–98
[23] Devlin B A and Corish J 1987 *J. Phys. C: Solid State Phys.* **20** 705–21
[24] Corish J 1989 *J. Chem. Soc. Faraday Trans.* 2 **85** 437–56
[25] Baetzold R C, Catlow C R A, Corish J, Healy F M, Jacobs P W M, Leslie M and Tan Y T 1989 *J. Phys. Chem. Solids* **50** 791–800
[26] Kirchhoff F, Holender J M and Gillan M J 1994 *Phys. Rev.* B **49** 17420–3
[27] Onwuagba B N 1996 *Solid State Commun.* **97** 267–71
[28] Vogel D, Krüegr P and Pollmann J 1998 *Phys. Rev.* B **58** 3865–9
[29] Nunes G S, Allen P B and Martins J L 1998 *Solid State Commun.* **105** 377–80
[30] Victora R H 1997 *Phys. Rev.* B **56** 4417–21
[31] Ves S, Glötzel D, Cardona M and Overhof H 1981 *Phys. Rev.* B **24** 3073–85
[32] Kunz A B 1982 *Phys. Rev.* B **26** 2070–5
[33] Aprà E, Stefanovich E, Dovesi R and Roetti C 1991 *Chem. Phys. Lett.* **186** 329–35
[34] Glaus S and Calzaferri G 2003 *Photochem. Photobiol. Sci.* **2** 398–401
[35] Baetzold R C and Eachus R S 1995 *J. Phys.: Condens. Matter* **7** 3991–9
[36] Shluger A L, Foster A S, Gavartin J L and Sushko P V 2003 *Nano and Giga Challenges in Microelectronics* ed J Greer, A Korkin and J Labanowski (Amsterdam: Elsevier) pp 151–222

[37] Pacchioni G, Frigoli F, Ricci D and Weil J A 2000 *Phys. Rev.* B **63** 054102
[38] Gavartin J L, Sushko P V and Schluger A L 2003 *Phys. Rev.* B **67** 035108
[39] Segall M D, Lindan P J D, Probert M J, Pickard C J, Hasnip P J, Clark S J and Payne M C 2002 *J. Phys.: Condens. Matter* **14** 2717–44
[40] Perdew J P, Burke K and Ernzerhof M 1996 *Phys. Rev. Lett.* **77** 3865–8
[41] Koelling D D and Harmon B N 1977 *J. Phys. C: Solid State Phys.* **10** 3107–14
[42] Simard B, Hackett P A, James A M and Langridge-Smith P R R 1991 *Chem. Phys. Lett.* **186** 415–22
[43] Ran Q, Schmude R W, Gingerich K A and Wilhite D W 1993 *J. Phys. Chem.* **97** 8535–40
[44] Lide D R (ed) 2002–2003 *Handbook of Chemistry and Physics* 83rd edn (Boca Raton, FL: CRC Press)
[45] Huber K P and Herzberg G 1979 *Molecular Spectra and Molecular Structure Constants of Diatomic Molecules* (New York: Van Nostrand-Reinhold)
[46] Hildenbrand D L and Lau K H 1996 *High Temp. Mater. Sci.* **35** 11–20
[47] Schultz P A 2000 *Phys. Rev. Lett.* **84** 1942–5
[48] Makov G, Shah R and Payne M C 1996 *Phys. Rev.* B **53** 15513–7
[49] Leslie M and Gillan M J 1985 *J. Phys C: Solid State Phys.* **18** 973–82
[50] Kleinman L 1981 *Phys. Rev.* B **24** 7412–4
[51] Laks D B, Van de Walle C G, Neumark G F, Blöchl P E and Pantelides S T 1992 *Phys. Rev.* B **45** 10965–78
[52] Roma G and Limoge Y 2003 *Nucl. Instrum. Methods* B **202** 120–4
[53] Bucher M 1987 *Phys. Rev.* B **35** 6432–4
[54] Stoneham A M 1975 *Theory of Defects in Solids* (Oxford: Oxford University Press)
[55] Gale J D 1997 *J. Chem. Soc., Faraday Trans.* **93** 629–37
[56] Shukla A K, Ramdas S and Rao C N 1973 *J. Solid State Chem.* **8** 120–5
[57] Weber M D and Friauf R J 1969 *J. Phys. Chem. Solids* **30** 407–19
[58] Eachus R S, Pawlik T D and Baetzold R C 2000 *J. Phys.: Condens. Matter* **12** 8893–911
[59] Delley B 2000 *J. Chem. Phys.* **113** 7756
[60] Perdew J P and Wang Y 1992 *Phys. Rev.* B **45** 13244–9
[61] Sushko P V 2000 Development and application of embedded cluster methodologies for defects in ionic materials *PhD Thesis* The Royal Institution of Great Britain
[62] Shannon R D 1976 *Acta Crystallogr.* A **32** 751